Simulation of carrier transport in heterostructures using the 2D self-consistent full-band ensemble Monte Carlo method*

Wei Kangliang(魏康亮), Liu Xiaoyan(刘晓彦), Du Gang(杜刚)†, and Han Ruqi(韩汝琦)

(Institute of Microelectronics, Peking University, Beijing 100871, China)

Abstract: We demonstrate a two-dimensional (2D) full-band ensemble Monte–Carlo simulator for heterostructures, which deals with carrier transport in two different semiconductor materials simultaneously as well as at the boundary by solving self-consistently the 2D Poisson and Boltzmann transport equations (BTE). The infrastructure of this simulator, including the energy bands obtained from the empirical pseudo potential method, various scattering mechanics employed, and the appropriate treatment of the carrier transport at the boundary between two different semiconductor materials, is also described. As verification and calibration, we have performed a simulation on two types of silicon–germanium (Si–Ge) heterojunctions with different doping profiles—the p–p homogeneous type and the n–p inhomogeneous type. The current–voltage characteristics are simulated, and the distributions of potential and carrier density are also plotted, which show the validity of our simulator.

Key words: heterostructure; Monte Carlo simulation; carrier transport
DOI: 10.1088/1674-4926/31/8/084004 **PACC:** 7340L; 7430F; 7115Q

1. Introduction

As a promising device architecture, semiconductor heterostructures have drawn much interest. Over the past years, several kinds of heterostructure devices have been in industrial manufacture, such as the heterojunction bipolar transistor (HBT) for high-speed, high-linearity and low-noise applications, the modulation-doped field effect transistor (MODFET) for analogue microwave applications, and many other heterostructure devices for optoelectronic applications[1]. In particular, as the gate lengths of MOSFETs are reduced to below 100 nm in the aggressive scaling-down process, a number of problems have arisen, and one of the most significant is the reduction of electron and hole mobilities in the inversion layers of MOSFETs caused by the increasing probability of scattering with semiconductor–insulator boundaries due to the reduction of the gate insulator thickness[2]. The band structure and strain engineering introduced by Si/SiGe heterostructure is one of the leading method of substantially improving the carrier mobilities in the inversion layers of MOSFETs[3, 4].

The great advantage of fabricating various heterostructure devices calls for a detailed understanding of carrier transport in semiconductor heterostructures, which is a prerequisite for designing and optimizing devices based on this architecture. For a deep investigation, the Monte Carlo method is well known as a powerful tool for the study of carrier transport phenomena in a large variety of semiconductor materials and devices. So far, a great deal of work has been devoted to the Monte Carlo simulation of carrier transport in heterostructure devices of various material systems[5−23]. Nevertheless, most of the simulations have focused on the study of strain-induced improvements of carrier mobilities in Si/SiGe systems[5−9] and the carrier transport properties of two-dimensional electron gas (2DEG) confined in heterostructure barriers[10−23]; little work has been done on the study of carrier transport across two different semiconductor materials in heterostructures, which is essential in understanding the physical phenomena and processes occurring in various advanced semiconductor structures.

Compared to conventional ones, it is more difficult to develop a Monte Carlo simulator for heterostructures. The following points indicate the two most significant problems: (1) First is the proper maintenance of two different sets of scattering parameters and band structures without too much overhead in simulation, which will be even more serious when constructing a full-band simulator, just as is the case in this work. (2) The second is the close monitoring of carrier movements in different semiconductor materials, where appropriate treatment is required when a carrier is about to travel from one semiconductor material into another at the boundaries.

The purpose of this paper is to present in detail the infrastructure and models of a 2D self-consistent full-band ensemble Monte Carlo simulator for heterostructures, which is based on our former simulator for the single semiconductor material Si or Ge[24, 25]. In the following, we describe the full-band model and scattering mechanisms employed, present the flow of our Monte Carlo simulator for heterostructures, and in particular the proper treatment needed for multiple semiconductor materials and the carrier transport at the boundary between them, and give the simulation results of two types of Si–Ge heterojunctions to verify our simulator.

2. Physical model

The full-band structures used in our Monte Carlo simulator are obtained through the local empirical pseudo-potential

* Project supported by the National Fundamental Basic Research Program of China (No. 2006CB302705) and the Foundation for Key Program Project of Chinese Ministry of Education (No. 107003).
† Corresponding author. Email: gang_du@ime.pku.edu.cn
Received 16 January 2010, revised manuscript received 18 March 2010 © 2010 Chinese Institute of Electronics

Table 1. Phonon scattering parameters for electrons and holes in Si and Ge[27].

Carrier type	Parameter	Si	Ge	Unit
Electron	Deformation potential for elastic acoustic phonon	8.7	13.0	eV
	Deformation potential constant for TA (g_1)	0.47	0.2	10^8 eV/cm
	Phonon temperature for TA (g_1)	140	120	K
	Deformation potential constant for LA (g_2)	0.74	4.0	10^8 eV/cm
	Phonon temperature for LA (g_2)	215	320	K
	Deformation potential constant for LO (g_3)	10.2	2.6	10^8 eV/cm
	Phonon temperature for LO (g_3)	720	430	K
	Deformation potential constant for TA (f_1)	0.28		10^8 eV/cm
	Phonon temperature for TA (f_1)	220		K
	Deformation potential constant for LA (f_2)	1.86		10^8 eV/cm
	Phonon temperature for LA (f_2)	550		K
	Deformation potential constant for TO (f_3)	1.86		10^8 eV/cm
	Phonon temperature for TO (f_3)	685		K
Hole	Deformation potential for elastic acoustic phonon	9.3	3.5	eV
	Deformation potential constant for optical phonon	4.0	4.1	10^8 eV/cm
	Phonon temperature for optical phonon	680	430	K

method with spin-orbit interaction included[26]. Four conduction bands and three valence bands have been calculated for each semiconductor material. For Si and Ge in particular, some of the material parameters important for the following simulation are the same as those in Ref. [27].

The scattering rates for the various scattering processes are calculated with Fermi's golden rule:

$$\Theta(k,k') = \frac{2\pi}{\hbar} \mid H_{k'k} \mid^2 \delta(\varepsilon_{k'} - \varepsilon_k - \varepsilon_{k'k}). \quad (1)$$

In our simulator for heterostructures, the following scattering mechanisms are included: acoustic and optical phonon scattering with both intravalley and intervalley transition, ionized impurity scattering and impact ionization scattering. The interaction between phonons and electrons and holes is described in the deformation-potential approach as presented by Jacoboni *et al.*[27]. In the case of electrons, the acoustic intravalley phonon scattering is assumed to be elastic for both Si and Ge. Six Δ–Δ intervalley scattering processes for Si and three intervalley scattering processes (L–L, L–Δ and Δ–Δ) for Ge are considered. In the case of holes, only the elastic acoustic phonon and one type of optical phonon are considered (see Table 1). Ionized impurity scattering is treated via the screened Coulomb potential in the Brooks–Herring approach[27]. The scattering rate of impact ionization is dependent on energy[28], and the final energy after scattering is determined by the method proposed by Kunikiyo *et al.*[29].

3. Self-consistent Monte Carlo scheme for heterostructures

The Poisson equation employed in our simulator can be written as

$$\nabla \cdot (\varepsilon \nabla \Psi) = -\rho, \quad (2)$$

where ε is the dielectric constant, Ψ is the electrostatic potential, and ρ is the charge density. In heterostructures, the Poisson equation requires no special change as long as the various relative dielectric constants for different semiconductor materials are considered. The carrier transport is described with the BTE below:

$$\left[\frac{\partial}{\partial t} + v(k)\nabla_r + \left(\frac{\mathrm{d}k}{\mathrm{d}t}\right)\nabla_k\right] f(r,k,t) = \frac{\Omega}{(2\pi)^3} \int \left[f(k',t)\Theta(k',k) - f(k,t)\Theta(k,k')\right] \mathrm{d}k', \quad (3)$$

where v is the velocity of the carrier, $f(r,k,t)$ is the single particle distribution function which gives the probability for the occupation of a particle state, Ω is the real space volume, and $\Theta(k,k')$ is the scattering rate described by Eq. (1). The BTE described by Eq. (3) is a linear equation because we have neglected the effect of Pauli's exclusion principle on the assumption that the particle gas is dilute enough for us to ignore the particle–particle interaction.

Once the initial state of the system is set, the Poisson equation is solved throughout the whole device at the beginning of each time step. Then the duration of a free flight is chosen stochastically for each particle with a probability distribution determined by the various scattering probabilities. The free flight is applied to the particle with the existence of an external electric field calculated in the former solution of the Poisson equation. At the end of the free flight, a scattering is chosen and the final state of the particle after scattering is randomly determined according to the particular selection rule. Next, the entire process is repeated. By this method, the 2D Poisson equation and Boltzmann equation are solved self-consistently. To improve the statistical efficiency, the phase space multiple refresh method[28] is used.

One most significant difference between our Monte Carlo simulator for heterostructures and a conventional one is that different scattering and band systems are applied to carriers in different semiconductor materials. These various bands and scattering systems are stored separately in a form that can be easily retrieved in simulation to save CPU time. In addition, to apply the correct band and scattering system to a particle, an extra index is needed for every particle to tell which semiconductor material it is in, which will lead to a significant computational time increase when the total particle number is large.

Another problem arises when a carrier reaches the boundary between two semiconductor materials and is about to travel

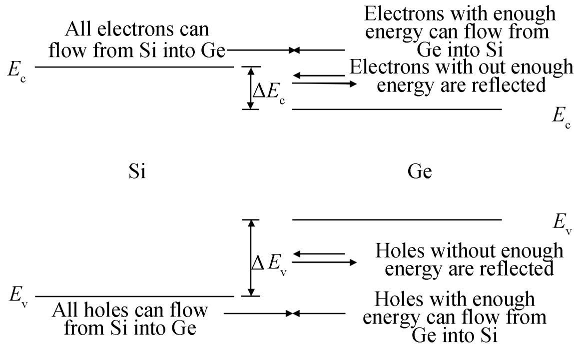

Fig. 1. Illustration for different cases of carriers traversing the material interface between Si and Ge.

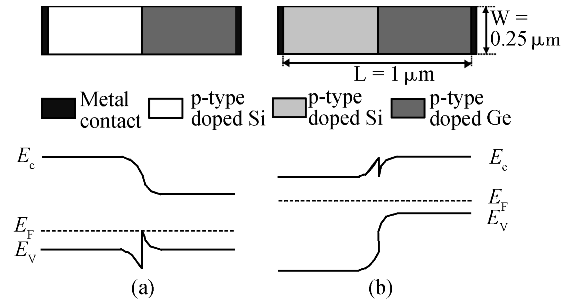

Fig. 2. Schematic sketch of the heterojunctions simulated in this work and their equilibrium energy band diagram. (a) p–p homogeneous type Si–Ge heterojunction. (b) n–p heterogeneous type Si–Ge heterojunction.

across it. Different models can be used to treat this kind of transport, and the simplest one is the thermoionic emission model as employed in the demonstration simulation in Section 4. However, other sophisticated models can also be easily included in our simulator. For the thermoionic emission model, the conservation of energy must be fulfilled at the interface:

$$\varepsilon_1(k_1) = \varepsilon_2(k_2), \tag{4}$$

where k_1 is the particle state on one side of the interface and k_2 the state on the other side. Because of the discontinuity of the band edges of Si and Ge, carriers that traverse across the material boundary from Si to Ge are different from those from Ge to Si. The carriers at the Ge side of the boundary will flow into Si only when they have enough energy to surmount the barrier, otherwise they are reflected. For electrons the minimum energy is ΔE_c, and for holes it is ΔE_v, where ΔE_c and ΔE_v are the discontinuities of the conduction and valence band edges respectively. However, the carriers at the Si side of the boundary will all flow into Ge (Fig. 1). Once a carrier has traversed across the material boundary, the particle state after the transition is found by a search for a stochastic state with the correct energy with

$$v_{1,\perp}(k_1)v_{2,\perp}(k_2) \geqslant 0 \tag{5}$$

to ensure that the particle moves into the new material, where $v_{i,\perp}(k_i)$ $(i = 1, 2)$ is the velocity component perpendicular to the material interface. Although this transport model is rather simple, it does provide some meaningful results that we will discuss in the next section.

4. Simulation results

A p–p Si–Ge heterojunction and an n–p Si–Ge heterojunction are simulated in this work to verify the simulator, and schematic sketches as well as an equilibrium energy band diagram are plotted in Fig. 2. The devices are in the shape of rectangles with the length $L = 1$ μm and the width $W = 0.25$ μm. Each of the two devices consists of two halves that are made of Si and Ge respectively. The doping concentration is chosen to be 10^{16} cm^{-3} for both donors and acceptors. A metal contact is placed at each end of the device for applying external voltages. The system temperature is set to be 300 K. The distribution of carrier and potential as well as the I–V curves are simulated.

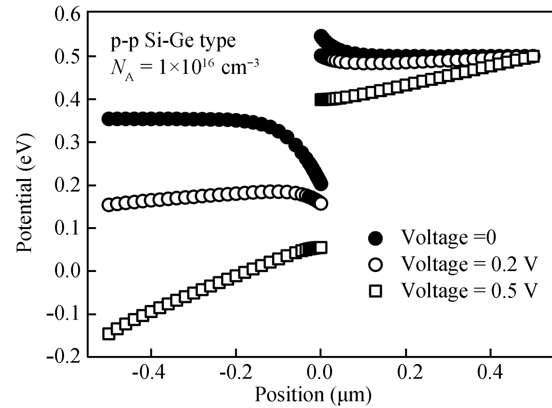

Fig. 3. Potential distribution along the lengthwise direction for a p–p Si–Ge heterojunction at varying external voltages. The discontinuity of the valence-band maxima is also shown.

4.1. p–p Si–Ge heterojunction

Figure 3 shows the potential distribution along the lengthwise direction for the p–p Si–Ge heterojunction at varying external voltages. The discontinuity of the valence-band maxima is also shown. Figure 4 shows the simulated hole density distribution with various bias voltages 0, 0.2 and 0.5 V. We can see that near the boundary of Si and Ge holes are depleted on the Si side and accumulate on the Ge side due to the discontinuity of the valence-band maxima as shown in Fig. 3. As the voltage increases, the depletion and accumulation phenomena of holes are weakened. Figure 5 shows the current–voltage curve of the p–p Si–Ge heterojunction, and the ambipolar feature resembling that of a p–n junction is successfully reproduced. It is shown in Fig. 5 that the current is relatively large when a forward bias is applied, but small when a reverse bias is applied. The large fluctuation of the current in the reverse-bias region is due to the great intrinsic noise of the Monte Carlo method.

4.2. n–p Si–Ge heterojunction

Figure 6 shows the potential distribution along the lengthwise direction for the n–p Si–Ge heterojunction at varying external voltages. The discontinuity of the conduction-band minima is considered. Figure 7 shows the electron and hole density distribution. It is shown that there is a slight accumulation of electrons on the Ge side of the boundary at large external volt-

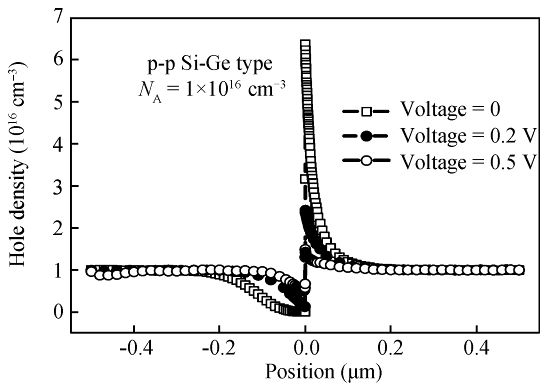

Fig. 4. Hole density distribution along the lengthwise direction for a p–p Si–Ge heterojunction at varying external voltages. Near the boundary of Si and Ge holes are depleted on the Si side and accumulate on the Ge side due to the discontinuity of the valence-band maxima.

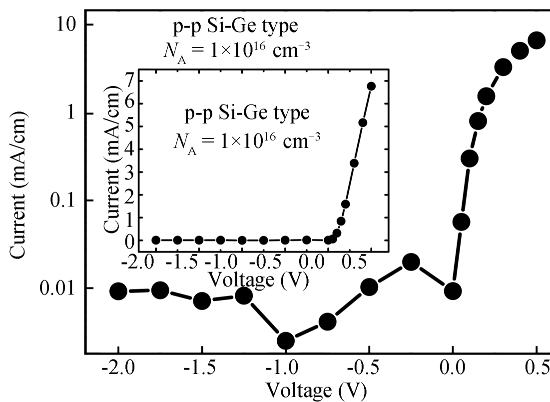

Fig. 5. Current versus external voltages for the p–p Si–Ge heterojunction.

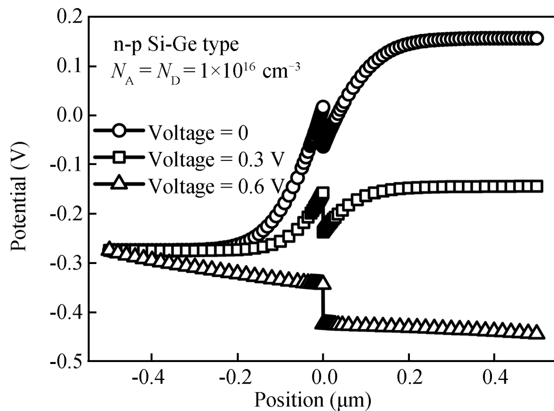

Fig. 6. Potential distribution along the lengthwise direction for an n–p Si–Ge heterojunction at varying external voltages. The discontinuity of the conduction-band minima is considered.

ages. This is because, when the external voltage is large enough (0.6 V in Fig. 7), the conduction-band minimum of Ge is lower than that of Si as shown in Fig. 6, and electrons will accumulate in that region. Figure 8 shows the current–voltage curve of the n–p Si–Ge heterojunction. Because of the great intrinsic noise

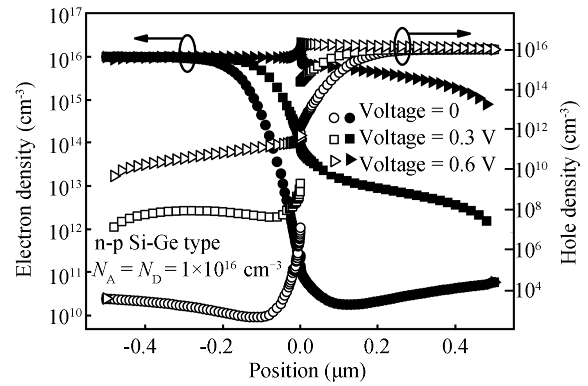

Fig. 7. Electron (solid symbols) and hole (open symbols) density distribution along the lengthwise direction for the n–p Si–Ge heterojunction at varying external voltages. There is a slight accumulation of electrons on the Ge side of the boundary at large external voltages (0.6 V in this figure).

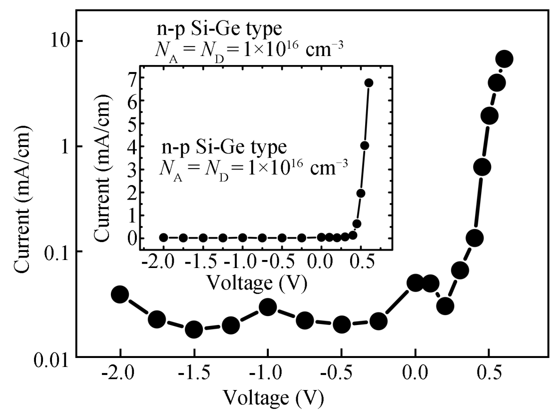

Fig. 8. Current versus external voltages for the n–p Si–Ge heterojunction.

of the Monte Carlo method, there is also a large fluctuation in the current, especially when the current is relatively small. This fluctuation cannot be eliminated by increasing the computation time.

5. Conclusion

A 2D full-band ensemble Monte Carlo simulator for heterostructures, which deals with carrier transport in two different semiconductor materials simultaneously as well as at the boundary by solving self-consistently the 2D Poisson and Boltzmann equations, is demonstrated in this paper. Based on the thermoionic emission model, we performed a sample simulation on two p–p and n–p Si-Ge heterojunctions as verification. The current–voltage characteristics, and the distributions of potential and carrier density are successfully simulated. These results show the validity of our simulator, and at the same time improve our insight into the microscopic operation of heterostructure devices.

References

[1] Douglas J P. Si/SiGe heterostructures: from material and physics to devices and circuits. Semicond Sci Technol, 2004, 19: 75

[2] Fischetti M V. Long-range Coulomb interactions in small Si devices. Part II. effective electron mobility in thin-oxide structures. J Appl Phys, 2001, 89: 1232

[3] Rim K, Hoyt J L, Gibbons J F. Fabrication and analysis of deep submicron strained-Si n-MOSFET's. IEEE Trans Electron Devices, 2000, 47: 1406

[4] O'Neill A G, Antoniadis D A. Deep submicron CMOS based on silicon germanium technology. IEEE Trans Electron Devices, 1996, 43: 911

[5] Aubry-Fortuna V,Dollfus P, Galdin-Retailleau S. Electron effective mobility in strained-Si/$Si_{1-x}Ge_x$ MOS devices using Monte Carlo simulation. Solid-State Electron, 2005, 49: 1320

[6] Bufler F M, Graf P, Keith S, et al. Full band Monte Carlo investigation of electron transport in strained Si grown on $Si_{1-x}Ge_x$ substrates. Appl Phys Lett, 1997, 70: 2144

[7] Dollfus P. Si/$Si_{1-x}Ge_x$ heterostructures: electron transport and field-effect transistor operation using Monte Carlo simulation. J Appl Phys, 1997, 82: 3911

[8] Roldan J B, Gamiz F , Lopez-Villanueva J A, et al. A Monte Carlo study on the electron-transport properties of high-performance strained-Si on relaxed $Si_{1-x}Ge_x$ channel MOSFETs. J Appl Phys, 1996, 80: 5121

[9] Demarina N V, Gruetzmacher D A. Low-temperature hole mobility in rolled-up Si/SiGe heterostructures. ASDAM, 2008: 91

[10] Ardaravicius L, Matulionis A, Liberis J, et al. Electron drift velocity in AlGaN/GaN channel at high electric fields. Appl Phys Lett, 2003, 83: 4038

[11] Monsef F, Dollfus P, Galdin-Retailleau S, et al. Electron transport in Si/SiGe modulation-doped heterostructures using Monte Carlo simulation. J Appl Phys, 2004, 95: 3587

[12] Oberheber R, Zandler G, Vogl P. Mobility of two-dimensional electrons in AlGaN/GaN modulation-doped field-effect transistors. Appl Phys Lett, 1998, 73: 818

[13] Yu T H, Brennan K F. Monte Carlo calculation of two-dimensional electron dynamics in GaN–AlGaN heterostructures. J Appl Phys, 2002, 91: 3730

[14] Polyakov V M, Schwierz F. Monte Carlo calculation of two-dimensional electron gas mobility in InN-based heterostructures. J Appl Phys, 2007, 101: 033703

[15] Li T, Joshi R P, Fazi C. Monte Carlo evaluations of degeneracy and interface roughness effects on electron transport in AlGaN–GaN heterostructures. J Appl Phys, 2000, 88: 829

[16] Thobel J L, Sleiman A, Bourel P, et al. Monte Carlo study of electron transport in III–V heterostructures with doped quantum wells. J Appl Phys, 1996, 80: 928

[17] Bhapkar U V, Shur M S. Monte Carlo calculation of velocity-field characteristics of wurtzite GaN. J Appl Phys, 1997, 82: 1649

[18] Reklaitis A, Grigaliunaite G. Monte Carlo study of DC and AC vertical electron transport in a single-barrier heterostructure. Phys Rev B, 2001, 63: 155301

[19] Rodilla H, Gonzalez T, Pardo D, et al. High-mobility heterostructures based on InAs and InSb: a Monte Carlo study. J Appl Phys, 2009, 105: 113705

[20] Toufik S, Jean-Luc T. Analysis of the high-frequency performance of InGaAs/InAlAs nanojunctions using a three-dimensional Monte Carlo simulator. J Appl Phys, 2009, 106: 083709

[21] Sadi T, Kelsall R W. Theoretical study of electron confinement in submicrometer GaN HFETs using a thermally self-consistent Monte Carlo method. IEEE Trans Electron Devices, 2008, 55: 945

[22] Ghaffari O, Saghafi K. Intersubband scattering effects on the carrier velocity of a AlGaAs/GaAs single-well heterostructure. INEC, 2008: 695

[23] Yoshihiro T, Hirofumi L, Hirokil F. Monte Carlo study of high-field electron transport characteristics in AlGaN/GaN heterostructure considering dislocation scattering. Physica Status Solidi C: Current Topics in Solid State Physics, 2007, 4: 2695

[24] Du G, Liu X Y, Han R Q. Quantum Boltzmann equation solved by Monte Carlo method for nano-scale semiconductor devices simulation. Chinese Physics, 2006, 15: 177

[25] Du G, Liu X Y, Xia Z L, et al. Monte Carlo simulation of p- and n-channel GOI MOSFETs by solving the quantum Boltzmann equation. IEEE Trans Electron Devices, 2005, 52: 2258

[26] Chelikowsky J R, Cohen M L. Nonlocal pseudopotential calculations for the electronic structure of eleven diamond and zinc-blende semiconductors. Phys Rev B, 1976, 14: 556

[27] Jacoboni C, Reggiani L. The Monte Carlo method for the solution of charge transport in semiconductors with application to covalent materials. Rev Mod Phys, 1983, 55: 645

[28] Thoma R, Peifer H J, Engl W L, et al. An improved impact-ionization model for high-energy electron transport in Si with Monte Carlo simulation. J Appl Phys, 1991, 69: 2300

[29] Kunikiyo T, Takenaka M, Kamakura Y, et al. A Monte Carlo simulation of anisotropic electron transport in silicon including full band structure and anisotropic impact-ionization model. J Appl Phys, 1994, 75: 297